IOP Publishing New J. Phys. 26 (2024) 103017 https://doi.org/10.1088/1367-2630/ad850e

New Journal of Physics
The open access journal at the forefront of physics

Deutsche Physikalische Gesellschaft DPG
IOP Institute of Physics

Published in partnership with: Deutsche Physikalische Gesellschaft and the Institute of Physics

OPEN ACCESS

RECEIVED
17 July 2024

REVISED
7 September 2024

ACCEPTED FOR PUBLICATION
9 October 2024

PUBLISHED
17 October 2024

PAPER

Prediction of ground state charge radius using support vector regression

Amir Jalili[1,2] and Ai-Xi Chen[1,*]

[1] Department of Physics, Zhejiang Sci-Tech University, Hangzhou 310018, People's Republic of China
[2] School of Physics, Nankai University, Tianjin 300071, People's Republic of China
[*] Author to whom any correspondence should be addressed.

E-mail: aixichen@zstu.edu.cn, jalili@zstu.edu.cn and jalili@nankai.edu.cn

Keywords: machine learning, support vector regression, RBF, charge radii

Supplementary material for this article is available online

Abstract

We systematically investigate the prediction of nuclear charge radii using a support vector regression (SVR) model in machine learning(ML), specifically employing a radial basis function (RBF) kernel. Our model is designed to capture the global structure of the radius surface through the utilization of feature spaces encompassing both (N, Z) and (N, Z, A). We achieved a root mean square deviation of 0.019 fm with respect to 885 measured charge radii ($Z \geqslant 8$). By incorporating the atomic mass number as an additional feature, the model successfully reproduces the charge radii of ($^{40-50}$Ca), ($^{74-96}$Kr), ($^{120-148}$Ba), and ($^{183-199}$Au) isotopes. Furthermore, our ML method demonstrated an extrapolation capability with a deviation of 0.016 fm relative to 10 022 calculated charge radii based on the Weizsacker–Skyrme model. The SVR model's performance is further tested across different regions of the charge radii table, demonstrating significant agreement with experimental data and underscoring the efficacy of the RBF kernel in nuclear charge radii prediction.

1. Introduction

Numerous theoretical approaches have been developed to predict nuclear charge radii. These range from simple liquid drop models [1, 2] and the Garvey–Kelson relation [3] to their more advanced versions, which consider isospin dependence and shell effects [4–8]. Other methods include phenomenological formulas [4], microscopic models such as the Skyrme-Hartree–Fock-Bogoliubov (HFB) models [9, 10], and the relativistic mean-field (RMF) model. Additionally, local-relation based models [6, 11, 12], sophisticated mean-field models [13–16], *ab initio* no-core shell models [17, 18], and the Weizsäcker–Skyrme (WS*) model [4] have been utilized. Experimental techniques to measure charge radii include charged particle scattering, laser spectroscopy, muonic atom x-ray, K_α, and optical isotope shift methods [19–21].

Several interesting phenomena and challenges persist, such as the unexpected increase in charge radii for neutron-rich Calcium isotopes [22, 23], the end of shape staggering in Mercury isotopes [24], and the odd–even staggering in proton-rich Calcium isotopes [25]. To address these challenges and explore new experimental data, it is essential to adopt advanced techniques.

Machine learning (ML) models have emerged as powerful tools for predicting charge radii [26–30]. These models are capable of handling complex systems and providing fast, accurate predictions, thus accelerating computational efforts. The application of ML in physics has yielded significant insights across various domains [31–41]. Incorporating ML into nuclear physics represents a transformative approach that refines theoretical models and reduces uncertainties in charge radii predictions.

Among the effective ML techniques are kernel ridge regression (KRR) [42] and radial basis function (RBF) methods [43, 44]. Our approach diverges from traditional kernels and networks such as Bayesian neural networks and standard neural networks (NNs) by utilizing the support vector machine (SVM) model to improve charge radii predictions. Support vector regression (SVR) has emerged as a powerful tool in ML

for its ability to handle high-dimensional data and maintain robustness in predictions. Developed by Vapnik [45, 46], this regression is grounded in the principle of structural risk minimization [47], which aims to find a balance between model complexity and prediction accuracy, thereby minimizing the generalization error. SVM dynamically interacts with NNs to optimize weights, vectors, and other parameters, enhancing the accuracy of nuclear charge radii predictions. This novel application of SVR to nuclear structure represents a significant advancement over conventional methods and highlights the versatility of ML techniques in deepening our understanding of nuclear properties.

This paper is structured as follows: In section 2, we describe the construction of the refined SVR model, including feature selection and data segmentation. We demonstrate RBF in SVR and model description in sections 3 and 2.2. We demonstrate the efficacy of our method by applying it to the isotopes of Calcium ($^{40-50}$Ca), Krypton ($^{74-96}$Kr), Barium ($^{120-148}$Ba), and Gold ($^{183-199}$Au). Results and discussions are presented in section 3, followed by a summary and outlook in section 4.

2. Theory

In alignment with the approaches outlined in [27–30], our objective is to combine a theoretical model of charge radii with regression tools to enhance the characterization of nuclear charge radii. In our methodology, SVR is employed to model the residuals between theoretical predictions and corresponding experimental data. Subsequently, we elucidate our selection process for the theoretical model and expound on the construction of the network. Diverging from the conventional feed-forward NNs, which deterministically optimize complex, non-linear mappings between input features ($\boldsymbol{x}$) and outputs ($\boldsymbol{y}$), our model harnesses the power of network regression. The SVR model introduces a unique advantage by framing nuclear data as features derived from suggestions based on the global structure of the radius surface. For constructing our network, we employ data obtained from the framework of the radius surface formula [48] as features ($\boldsymbol{x}$) within feature spaces. As highlighted in the Introduction, an array of microscopic and macroscopic models have been utilized to elucidate atomic nuclei, with many providing reasonably accurate descriptions of nuclear charge radii [7, 49]. While macroscopic models offer practical convenience, microscopic models such as the RMF model [49] are computationally intensive yet encapsulate richer physical insights. However, for the current study, we select to integrate an isospin-dependent formula developed by Nerlo-Pomorska and Pomorski [50]. The radius surface formula embodies a formulation that incorporates various bulk properties such as N, Z, and A, with adjustable parameters such as r_a, b, and c.

Utilizing the isospin-dependent radius surface formula and these coefficients, the charge radii are determined by the equation (1):

$$R(Z,A) = r_a A^{1/3}\left[1 - b\frac{(N\text{-}Z)}{A} + \frac{c}{A}\right], \tag{1}$$

where $r_a = 0.98$, $b = 0.24$, and $c = 0.59$ represent the extracted parameters in our calculations, consistent with prior findings [51]. Employing least square fitting, the root mean square error (Rmse) for approximately 885 nuclei ($Z \geqslant 8$) is approximately 0.092 fm. Our objective is to utilize SVR to diminish this deviation.

2.1. RBF in SVR

In optimization problems, SVRs serve dual purposes in both classification and regression tasks [52]. In the context of SVR, the provided features, denoted as (N,Z,A) and (N,Z), represent data points, each categorized into one of two classes. We will investigate the specifics of these features shortly, with visual aids provided in figure 1. In the SVR model, both classification and regression can be performed for a given dataset. However, in our scenario, we are solely concerned with regression tasks. The objective is to determine the class of a new data point based on its features. In this model, each data point is viewed as a p-dimensional vector, and the goal is to find a $p-1$ dimensional hyperplane that effectively separates the data points into distinct classes. This hyperplane acts as a linear classifier, with the optimal hyperplane being the one that maximizes the separation or margin between classes [45].

Any hyperplane can be represented as the set of vector points $\boldsymbol{x}$ satisfying the equation $w \cdot \boldsymbol{x} - b = 0$, where xw is the weight vector. Consider a training dataset denoted as $(\boldsymbol{x}_1, y_1), \ldots, (\boldsymbol{x}_P, y_P)$, sampled from a function $y = f(\boldsymbol{x})$, where $\boldsymbol{x}$ represents the input variable (with one set for (N,Z) values and another set for (N,Z,A) values), constituting a vector of dimension. The corresponding output variable, y, is a unique real number associated with a given $\boldsymbol{x}$. In our analysis, the input vector $\boldsymbol{x}$ is constructed from multiple components, including N, Z, and A based on the radius surface formula, while y corresponds to the charge radii R. The SVM formulation involves solving an optimization problem with the objective function:

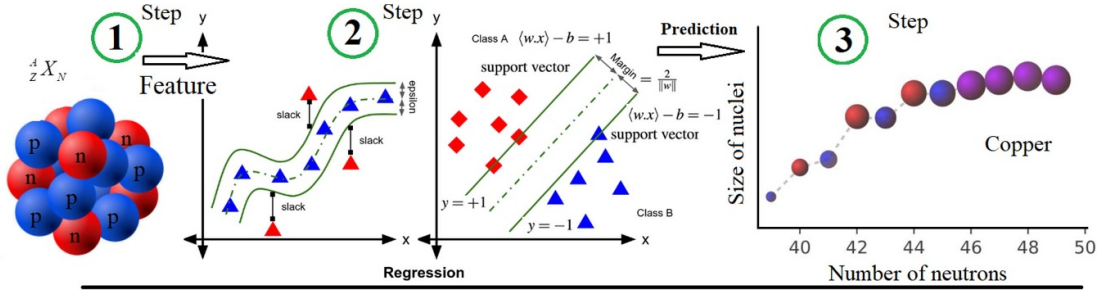

Figure 1. Schematic representation of the adjustable SVR structure utilized in this study.

$$\text{minimize} \quad \left(\frac{1}{2}\|w\|^2 + C\sum_{i=1}^{l}(\xi_i + \xi_i^*)\right), \tag{2}$$

subject to $y_i - (w\boldsymbol{x}_i) - b \leqslant \epsilon + \xi_i$, $(w\boldsymbol{x}_i) + b - y_i \leqslant \epsilon + \xi_i^*$, and $\xi, \xi_i^* \geqslant 0$ with $C > 0$. The notation $\|\|$ represents the Euclidean norm of a vector. The variables ξ_i and ξ_i^* are slack variables, measuring the error for the input and output $(\boldsymbol{x}_i, y_i)$ pairs. The hyperparameter ϵ specifies the tolerance margin for errors during training. These optimization approaches aim to minimize deviations from the predictions of SVR, particularly as applied to nuclear masses [45–47]. The RBF kernel stands as a versatile choice, adept at capturing intricate patterns in the data. It is defined as:

$$K_{\text{RBF}}\left(x_i, x_j\right) = \exp\left(-\gamma\|x_i - x_j\|^2\right), \tag{3}$$

where γ controls the width of the Gaussian function. The formulation of nuclear charge radii in this study employs a ML approach using the SVR model, which differs fundamentally from traditional empirical formulas. While empirical relations such as equation (1) offer valuable physical insights into the isospin asymmetry effects, the SVR model instead focuses on directly predicting charge radii from input features using kernel methods. In particular, the RBF kernel, as defined in equation (3), is utilized, which is well-suited for capturing the non-linear and complex relationships present in nuclear data. The RBF kernel effectively maps the input features N, Z, and A into a higher-dimensional space where the SVR model can recognize intricate patterns. This approach allows us to predict charge radii or predefined functional forms. The RBF kernel serves as a flexible tool, enabling the SVR model to capture subtle variations in nuclear structure across isotopes, even in regions with significant isospin asymmetry. By abstracting from physical models and focusing purely on the predictive performance of ML, our method offers a novel approach to understanding and predicting nuclear charge radii.

In this study, the SVR method was employed to assess the predictive performance and quantify the uncertainty in charge radii estimations. The uncertainty in our ML model is characterized using the Rmse, which represents the deviation between experimental and predicted charge radii. The Rmse serves as a key metric for evaluating the model's reliability. Mathematically, it is defined as:

$$\sigma_{\text{Rmse}} = \sqrt{\frac{1}{n}\sum_{i=1}^{n}\left(R_i^{\text{exp}} - R_i^{\text{th}}\right)^2}, \tag{4}$$

where R_i^{exp} and R_i^{th} are the experimental and predicted charge radii, respectively, and n is the number of data points. This approach allows us to quantify the overall uncertainty in our predictions, providing a robust measure of model performance.

2.2. Model description

In our base model, denoted as (NZ), the input feature space includes the number of neutrons N and the number of protons Z, with the sole prediction being the nuclear charge radii. For (NZA), we incorporate additional bulk properties, including the mass number A. In the training process of the SVR, the experimental data is taken from the AME2020 [53], and the theoretical data regarding extrapolation capability is taken from the WS* and HBF25 mass table [4, 9]. When using ML models to predict nuclear properties, the selection of input features is a critical factor. In our study, we utilized both the NZ and NZA feature sets, treating the mass number ($A = N+Z$) as an additional independent feature. While A is a linear combination of$N$ and$Z$, including it enhances the model's ability to capture complex, non-linear interactions

that might be missed when using only N and Z. This enhancement was clear in our results, as the NZA feature set consistently outperformed the NZ set, resulting in a lower Rmse. It is important to note that in this study, we used the mass number as an input feature, rather than the nuclear mass. This approach avoids the complexities associated with employing theoretical or empirical mass models such as the AME. By doing so, we ensure that the model remains focused on structural properties and delivers reliable predictions across a wide range of isotopic chains. The difference in performance between the NZ and NZA feature sets highlights the potential for seemingly redundant features to improve the effectiveness of SVR in predicting nuclear charge radii. The AME2020 dataset includes 885 measured charge radii ($Z \geqslant 8$), while for extrapolation candidates, 10 022 nuclei for (WS*) and 9484 nuclei for HFB25 have been selected to predict the charge radii. In this study, we selected theoretical models for benchmarking and integration with the SVR approach based on their renowned accuracy and extrapolative reliability across a wide range of nuclear isotopes. Specifically, the WS* and HFB25 models were chosen for their universal predictive precision. Our methodology involves incorporating predictions from these models into the training dataset, enabling the SVR to learn from both experimental measurements and theoretical estimates. This results in a regression model capable of accurately predicting charge radii, even in regions with limited or no experimental data, as evidenced by the consistent Rmse values observed during extrapolation.

The feature selection process was crucial in improving the SVR model's ability to predict nuclear charge radii. We assessed features based on their relevance to nuclear properties and their impact on model accuracy. To guide our selection, we used the isospin-dependent radius surface formula, which considers the relationship between nuclear charge radii and the isospin of the nucleus. These fundamental parameters characterize nuclear structure and influence the distribution of nuclear matter. To validate the relevance of these features, we used statistical analysis and cross-validation techniques. First, we conducted correlation analysis to assess the relationship between each feature and the target variable (nuclear charge radius). Any features showing a strong correlation were considered potentially relevant. We then conducted a series of experiments using the SVR model, gradually adding and removing features to observe changes in the model's Rmse. This iterative process helped us identify the best features that resulted in the lowest Rmse, indicating the highest predictive accuracy. To ensure the best performance, we employed cross-validation techniques. By dividing the dataset into training and testing sets, we verified that the model's performance was consistent and not overfit to any specific subset of data. The features were validated based on their ability to consistently reduce prediction errors across different data subsets. Ultimately, we chose the final feature set, which included N, Z, and A. This set struck the best balance between model complexity and predictive accuracy. The proposed approach, with the RBF kernel, allowed the model to effectively generalize to unseen data while accurately capturing the underlying physical relationships described by the isospin-dependent radius surface formula.

2.3. Data segmentation

To ensure the effective training and evaluation of the SVR model, we employed a structured data segmentation strategy. The dataset was divided into training, validation, and test sets using different test size (ts) ranging from 0.1 to 0.3, with random states (RSs) set to 'default' and '1' for consistency and reproducibility. In other words, the test set could be from 10% to 30% of the total dataset, with the remaining data used for training and validation. The training set was allocated the majority of the data, allowing the model to learn the intricate relationships within nuclear charge radii. The validation set was crucial for tuning the model's hyperparameters, such as the RBF kernel parameters, and for selecting the optimal model configuration. Finally, the test set, which remained isolated during model training and validation, was used to assess the model's generalization ability and performance on unseen data. This segmentation strategy enabled a comprehensive evaluation of the SVR model across different nuclear regions and isotopic chains, ensuring that the results are reliable and applicable across diverse nuclear scenarios.

Training/Testing: To train and evaluate our SVR model for predicting nuclear charge radii, we systematically divided the dataset into training, validation, and test subsets. Specifically, we explored ts ranging from 0.1 to 0.3, meaning that 10%–30% of the data was used for testing, with the remainder for training and validation. This process was repeated for three different configurations: 10%, 20%, and 30% ts. Additionally, we varied the RS, setting it to both the default value and 1, to ensure the robustness of our results against different data splits. The RS is a parameter used to initialize the internal random number generator, ensuring reproducibility of the data splits. This approach allowed us to rigorously optimize the model's hyperparameters—regularization parameter C, Gaussian function width (γ), and margin (ϵ)—using grid search and random search techniques to minimize the errors. The model achieved an Rmse of 0.019 fm for the NZ and NZA feature set, demonstrating significant predictive accuracy. This comprehensive training and validation strategy highlights the SVR model's capability to accurately predict nuclear charge radii across

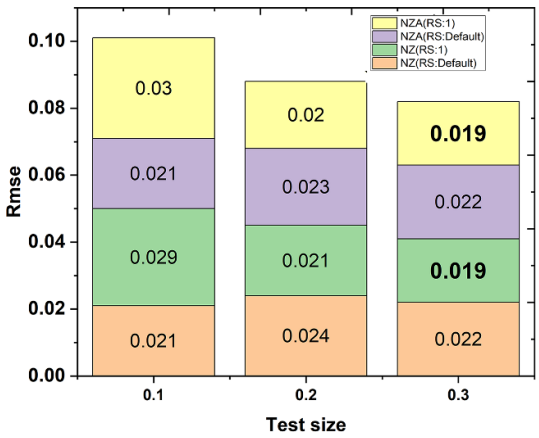

Figure 2. σ_{Rmse} based on different test sizes and random states (RS) for *NZ* and *NZA* features.

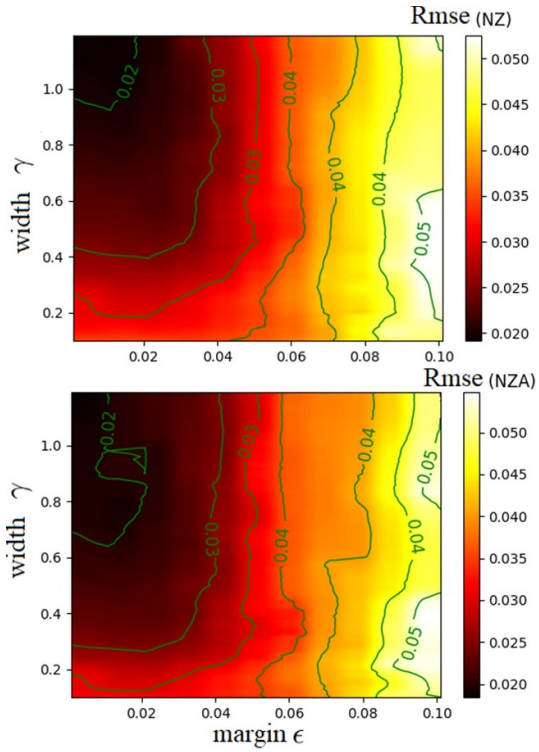

Figure 3. Variation of the Gaussian function width (γ) versus tolerance margin (ϵ) for $C = 1000$ during optimization of hyperparameters for charge radii.

various isotopic chains and extrapolation regions, emphasizing its efficacy and robustness. We will discuss this region later.

Given that our work involves a multidimensional feature space, we employed advanced techniques such as grid search and random search to fine-tune the hyperparameters and obtain σ_{Rmse}, as detailed in figure 2.

The impacts of the penalty term on the width of the Gaussian kernel are studied in detail in figure 3, where the 5-fold cross-validation is presented based on γ versus ϵ. So, the corresponding fewer deviations are clear around $\gamma = 1$. One can observe that the hyperparameters can be well-tuned according to the minima of the deviations. The resultant hyperparameters are shown in table 1, and the best corresponding performances regarding the deviations are 0.019 fm for both sets.

The SVR model offers several specific advantages over traditional methods in predicting nuclear charge radii. Firstly, the SVR model, especially when using the RBF kernel, achieves significantly higher predictive accuracy, as evidenced by a low Rmse of 0.019 fm for measured charge radii ($Z \geqslant 8$). This accuracy is notably superior to that of many traditional approaches. The model's ability to incorporate a broader feature space, including neutron number, proton number, and atomic mass number, allows it to capture the global

Table 1. Optimizing hyperparameters for the RBF kernel for nuclear charge radii.

Feature	Regularization Parameter	Other Parameters
(NZ)	$C = 4870$	$\gamma = 1, \epsilon = 0.01$
(NZA)	$C = 781$	$\gamma = 1, \epsilon = 0.001$

structure of the nuclear charge radii more effectively. This results in improved predictions across different isotopic chains and a strong capability to extrapolate to nuclei not included in the training set, as shown by an Rmse of 0.016 fm for extrapolated predictions. The choice of the RBF kernel is particularly advantageous because of its ability to handle complex, non-linear relationships within the data. This kernel function maps the input space into a higher-dimensional feature space, allowing the SVR model to learn the intricate dependencies between the features and the nuclear charge radii. The RBF kernel's flexibility and versatility make it well-suited to capture subtle variations in nuclear properties that linear models might miss. We tested various kernel functions and found that the RBF kernel provided the best performance, achieving a significantly lower root mean square deviation compared to other kernels. Our extensive testing of various kernels showed that the RBF kernel consistently resulted in the lowest Rmse, highlighting its effectiveness in accurately modeling the non-linear nature of nuclear charge radii. This careful selection of the RBF kernel significantly enhances the SVR model's performance, making it a powerful tool for predicting nuclear charge radii with high precision.

In this section, we will explore within the context of the SVR applied to the learning of residual charge radii differences between both features and experimental data and extrapolation region where the experimental data are unknown. To achieve this, we carefully prepared our testing sets, spanning the nuclear landscape from $Z \geqslant 8$ (^{16}O) to $Z = 96$ (^{248}Cm) for charge radii.

3. Results and discussion

Building upon previous research, such as the work conducted by Wang *et al* [4], we aim to further refine and advance SVR predictions. While deeper networks have demonstrated superior abilities in capturing intricate dataset complexities, our focus remains on simplicity and interpretability. Unlike deeper networks that may lack explicit insights into their training dynamics, our algorithm is intentionally designed to be concise, featuring only essential variables *N, Z*, and *A*, yet maintaining a high level of agreement between the testing set and SVR predictions.

As we progress, our strategy involves systematically augmenting the different ts from 0.1, 0.2 to 0.3 with the default RS and repeating the process with the RSe set to one to assess its impact on model performance. This iterative approach with varying configurations enables us to unravel the intricate interplay of various factors and optimize performance and their influence on predictive accuracy. Through this methodical investigation, we aim to strike a balance between model complexity and interpretability, unraveling the hidden complexities of nuclear charge radii predictions. We have identified the appropriate kernel in SVR to minimize deviation (lowest σ_{Rmse} of 0.019) for both sets, with a test size of 0.3 and a RS set to 1, as shown in figures 4 and 5.

This outcome suggests that this specific configuration provides the most accurate predictions for nuclear charge radii. Comparing these results with those obtained using only neutron number and proton number as features, we observe notable differences. The previous analysis with only *N and Z* features demonstrated a slightly higher σ_{Rmse}. This comparison underscores the enhanced predictive capability when incorporating both *N* and *Z* along with *A*, thereby improving the accuracy of the SVR model for nuclear charge radii predictions. Furthermore, we emphasize how SVR outperforms other sophisticated charge radii models or aligns with other ML techniques. The RBF kernel demonstrates a substantial improvement, achieving an impressive reduction in deviation. This meticulous progression highlights the significance of network engineering, displaying a tangible enhancement in predictive accuracy as we strategically vary ts. The choice of the best kernel function allows us to capture non-linear relationships within the data, potentially leading to better performance compared to other sophisticated models. This is particularly essential where the connection between features with the decision boundary (support vectors) and charge radii might not be perfectly linear. SVRs focus on feature data points closest to the support vectors. By prioritizing these crucial data points, SVRs can potentially achieve better generalizability to unseen data.

In our endeavor to minimize the σ_{Rmse} discrepancy between SVR predictions and experimental charge radii, a secondary objective is to explore specific mass regions. These regions comprehensively cover the charge radii within the training set, delineated by $2 \leqslant Z \leqslant 20$, $20 \leqslant Z \leqslant 50$, $50 \leqslant Z \leqslant 82$, $82 \leqslant Z$, and $16 \leqslant Z$. For each charge radii chain, results for the SVR calculations are reported under the best

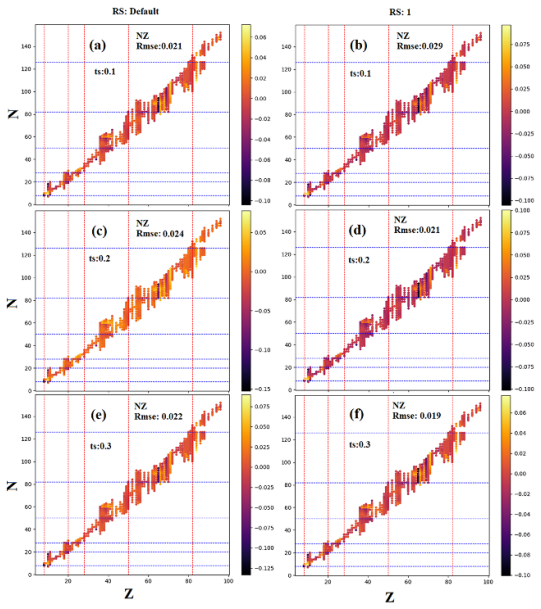

Figure 4. σ_{Rmse} between experimental and calculated values by SVR of the *NZ* system for different test sizes. The left and right panels represent the results obtained using the default and 1 random states, respectively.

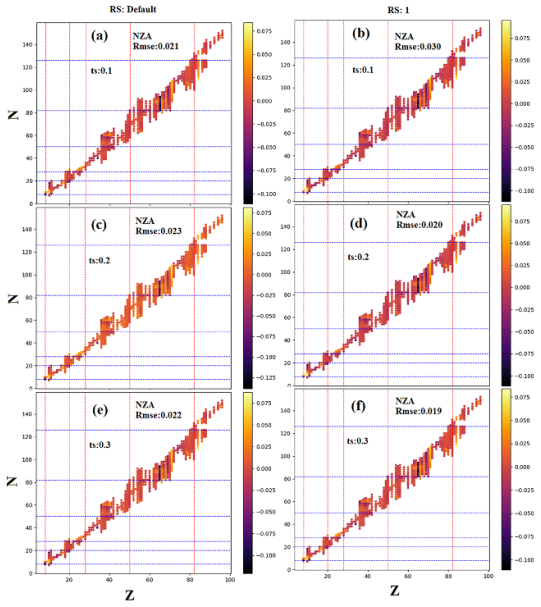

Figure 5. The same as figure 4, but for *NZA* system.

Table 2. SVR predictions for charge radii across diverse mass regions. Enhanced SVR performance is notable, particularly in the $20 \leqslant Z \leqslant 28$ in light mass nuclei.

Mass range	$8 \leqslant Z \leqslant 20$	$20 \leqslant Z \leqslant 28$	$28 \leqslant Z \leqslant 50$	$50 \leqslant Z \leqslant 82$	$82 \leqslant Z$	$50 \leqslant Z$	$28 \leqslant Z$	$20 \leqslant Z$	$8 \leqslant Z$
σ_{NZ}	0.053	0.177	0.009	0.021	0.002	0.016	0.016	0.019	0.019
σ_{NZA}	0.042	0.009	0.019	0.021	0.003	0.016	0.019	0.020	0.019

configuration for a test size of 0.3 and a RS set to one, considering the RBF kernel of *NZ* and *NZA* features, as summarized in table 2. The SVR model's performance is assessed using two feature sets: *NZ* and *NZA*, aiming to predict charge radii. The table underscores the SVR model's improved performance in the light mass region, particularly for nuclei with $8 \leqslant Z \leqslant 20$ and $20 \leqslant Z \leqslant 28$, where the σ_{NZA} is notably lower (0.009) compared to the σ_{NZ} (0.177). This suggests that the additional feature A enhances the model's ability to capture underlying patterns in nuclear charge radii. Across other mass regions, the *NZA* feature set

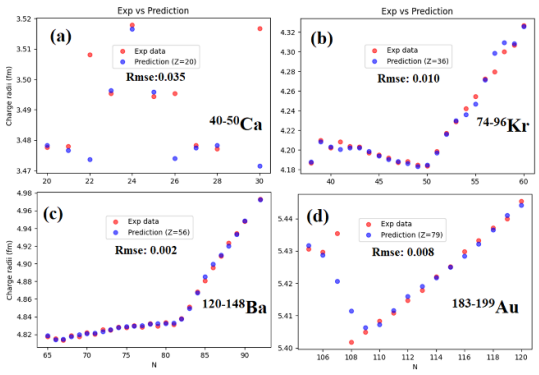

Figure 6. σ_{Rmse} between experimental and the calculated values by SVR of *NZA* system.

consistently maintains comparable or superior performance, especially for $8 \leqslant Z \leqslant 20$ and $20 \leqslant Z \leqslant 28$, highlighting its robustness in improving the SVR model's predictive accuracy across various mass regions. Support vectors, a reduced set of training patterns, determine the architecture and optimal number of neurons, functioning akin to a feedforward NNs. Unlike algorithms like backpropagation tailored for training systems, SVRs offer a broader approach, automatically determining suitable numbers of hidden units for charge radii prediction, regardless of the kernel choice. This adaptability distinguishes SVRs from traditional methods, allowing for more flexible architectures. Jian-Qin Ma *et al* employed KRR to refine the phenomenological nuclear charge radius formula [54], achieving a σ_{Rmse} of about 0.017 fm for 884 nuclei with $Z \geqslant 8$. Di Wu *et al* reported errors of 0.028 and 0.026 fm with and without the isospin effect in trained feed-forward NNs [30]. These results underscore the effectiveness of ML models in accurately predicting nuclear charge radii. Our regression's precision underscores the model's reliability and consistency, aligning with other ML predictions [30, 54] and demonstrating its potential in various nuclear physics research areas.

To assess SVR's robustness across the nuclear chart spectrum, ranging from light to heavy isotopes, we conducted a comparative analysis for specific elements - ($^{40-50}$Ca), ($^{74-96}$Kr), ($^{120-148}$Ba), and ($^{183-199}$Au) - compared to experimental data. This analysis, using the RBF kernel function and *NZA* configuration, revealed high predictive accuracy (as shown in figure 6). These isotopes studied here are known to exhibit nuclear deformation, which plays a significant role in determining charge radii. However, it is crucial to consider the potential impact of nuclear deformation and pairing correlations, especially in certain isotopes. Some of the isotopes we examined exhibit nuclear deformation, which significantly influences charge radii. Recent research by Geldhof *et al* [55] underscores the effects of nuclear deformation and pairing on charge radii, highlighting that deformation can lead to notable changes in radii. They have presented the calculated deformation energy curves, charge radii, and pairing gaps as functions of the quadrupole deformation parameter (β_2) for Pd and Pb isotopes. Their findings indicate that these isotopes exhibit a relatively soft deformation nature, as demonstrated by the shallow minima in the deformation energy curves. In our current methodology, the SVR model is trained exclusively on experimental charge radii data, which inherently includes deformation effects present in the measurements. Nevertheless, the model does not explicitly account for deformation parameters such as quadrupole deformation. Future research could enhance predictions by incorporating these deformation parameters as additional features, especially in regions where deformation is prominent. For the present study, our results assume spherical symmetry in the model's input features, which we acknowledge as a limitation in fully capturing the complexity of nuclear structure, particularly for deformed nuclei. Notably, the SVR model's predictions closely align with experimental values, with the lowest error observed for Ba isotopes. These results highlight the model's effectiveness across different isotopic chains, particularly in regions with high predictive accuracy.

Assessing a model's ability to extrapolate is vital across various applications. Although attaining a low σ_{Rmse} is relatively accessible for ML techniques, the true test of their extrapolation prowess lies in assessing their performance with experimental data that has not been employed during the training phase. This evaluation is crucial in ascertaining the effectiveness and adaptability of ML methods in real-world applications, where they are expected to make accurate predictions beyond the confines of their training data. To accurately evaluate various models, employing evaluation model data to compute σ_{Rmse} is imperative. The predictive skills of the current model for isotopes nearing the driplines, juxtaposed with established models like WS* [4], warrant careful examination. Explorations into nuclear properties, spanning from the proton drip line to the neutron drip line, have been conducted using diverse models, including deformed HFB theory [9] and nuclear density functional theory [56–59]. In this domain, our focus lies on evaluating the

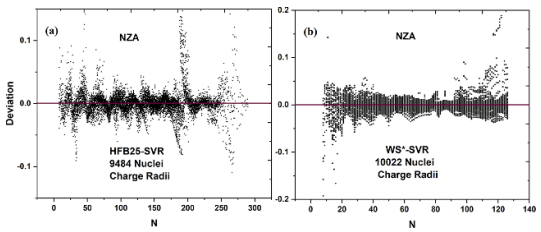

Figure 7. Deviation by SVR with WS [4] and HFB25 [9] in the *NZA* system.

Table 3. Extrapolation charge radii comparative analysis of σ_{Rmse} across various nuclear models, with values expressed in fm units.

Model	$A^{1/3}$	HFB25	WS*
This work	0.019	0.0210	0.016
Goriely *et al* [9]	1.48	0.0256	—
Li *et al* [7]	0.70	0.0254	0.021
Tang Zhang [26]	0.015	0.017	0.015
Ma *et al* [11]	—	0.024[a]	0.019

[a] σ_{Rmse} from HFB31. [11].

SVR's extrapolation performance. This entails venturing into regions beyond experimentally known boundaries to examine the SVR's capacity to generalize and make accurate predictions in unexplored territories. For comparative analysis of extrapolation capabilities, researchers have explored popular models such as $A^{1/3}$, WS* [4], and HFB25 [9] in ML. To facilitate comprehension, we present a comparison of σ_{Rmse} distribution across the training datasets in table 3, and charge radii differences are depicted in figure 7.

To assess the effectiveness of our SVR model in predicting nuclear charge radii, we compared it to several established nuclear mass models. Table 3 presents the σ_{Rmse} values for different models, including the empirical $A^{1/3}$ model, HFB25 [9], and WS* [7], as well as recent advancements [11, 26]. The results show that our SVR model, particularly when optimized with the RBF kernel, achieves an σ_{Rmse} of 0.019 fm for experimental data and an impressive 0.016 fm for extrapolation based on WS* predictions. Our model performs comparably to others, including HFB25, when comparing the reported Rmses. For instance, while the HFB25 model has an σ_{Rmse} of 0.0210 fm for similar datasets, our model's reduced error demonstrates the advantages of ML in capturing complex patterns in nuclear charge radii. This improvement is particularly evident when predicting charge radii in isotopes near the driplines, an area where traditional models often struggle. The results presented in table 3 highlight the strength of our approach and its potential as a valuable tool in nuclear structure studies, providing accurate predictions across a wide range of isotopes and nuclear mass regions.

A notable advantage of our SVR model lies in its ability to predict nuclear charge radii for isotopes that extend beyond the training dataset, particularly in areas close to the driplines where experimental data is limited. To evaluate this capability, we applied the model to several isotopes not included in the initial dataset. The findings indicate that the model can effectively extrapolate charge radii, achieving a σ_{Rmse} of less than 0.02 fm, which is in close agreement with theoretical predictions from models such as WS* and HFB25. This extrapolation ability is especially noticeable in light to medium-heavy nuclei, where the model adeptly captures exact trends in the radius surface as a function of neutron and proton numbers. Nevertheless, challenges might be in regions characterized by significant nuclear deformation or pairing effects, as our model does not explicitly incorporate these variables. Therefore, this restriction could produce considerable uncertainty in the predicted radii, particularly in the case of very heavy or neutron-rich isotopes, where intricate effects related to nuclear structure dominate. Future developments could focus on integrating deformation and pairing correlations to enhance the precision of these extrapolations.

Supplemental materials [60] include isotopes towards the driplines and comparisons with WS* and HBF25 [9]. Upon evaluating error metrics across four distinct models, it is apparent that the WS* model outperforms HBF25 and others. Comparisons between WS* [4], HBF25 [9], and SVR-calculated charge radii, particularly with the *NZA* feature of RBF kernel, reveal significant improvement. The overall agreement is substantial, with a σ_{RMSE} deviation of 0.016 fm for about 10 000 nuclei. The application of the RBF kernel in SVR markedly enhances the description of nuclear charge radii, highlighting the efficacy of the SVR method in predicting radii for unknown nuclei towards the driplines. To comprehensively illustrate these findings, results for different features in the RBF kernel are presented. These results underscore notable agreements between SVR predictions and experimental data. This detailed exploration underscores the

regression's ability, particularly in the *NZA* configuration, to capture and reproduce nuclear charge radii across a diverse range of masses. Overall, these investigations reaffirm the versatility and adaptability of SVR in modeling nuclear charge radii properties across varying elements and isotopes.

There are several promising directions for extending and refining this study. One approach is to incorporate pairing effects and nuclear deformation into the model. Additionally, exploring different kernel functions, such as polynomial or sigmoid kernels, could help model other nuclear properties like masses, binding energies, or quadrupole moments. While this study focused on specific isotopic chains, future research could expand the dataset to include more exotic isotopes, particularly those near the neutron and proton drip lines. Moreover, future studies could incorporate additional physical parameters, such as isospin asymmetry, neutron skin thickness, and higher-order moments, to further enhance predictive accuracy. These parameters are especially relevant for fine-tuning predictions in regions with strong collective effects. So, extending the model to account for pairing and deformation, testing additional kernel functions, and expanding the feature space to include more isotopes and physical parameters are all promising avenues for advancing ML approaches in nuclear physics.

The implications of our SVR model span multiple domains within nuclear physics and related fields, such as nuclear astrophysics and r-process phenomena, nuclear matter, and the equation of state. Additionally, our model offers efficiency and computational time savings compared to traditional microscopic approaches, which are often resource-intensive and time-consuming. The adaptability of the SVR framework enables it to predict a wide array of nuclear properties beyond charge radii, including quadrupole moments, decay rates, and mass distributions. This highlights the broader applicability of ML methods in nuclear physics, where these properties are crucial for understanding and modeling nuclear structures.

4. Conclusion

We applied SVR to train a model for describing charge radii, utilizing feature spaces encompassing neutron number, proton number, and atomic mass number configurations. The model performed well for both feature configurations, highlighting its versatility and effectiveness in capturing nuclear charge radius properties. Our study employed RBF kernel functions within SVR, resulting in a significant improvement in σ_{Rmse} compared to previous configurations. Specifically, σ_{Rmse} decreased from approximately 0.045 fm with only N, Z, and A numbers in the feature set to almost 0.016 fm when incorporating extrapolation possibilities for RBF kernels. This enhancement underscores the efficacy of incorporating additional features in improving predictive accuracy. An intriguing avenue for future exploration lies in investigating the expanded input feature space beyond the driplines, spanning from light to heavy nuclei. Our findings suggest that SVR offers a systematic and principled method for modeling charge radii. This compares with supervised learning approaches using MLPs or NNs trained through backpropagation or conjugate-gradient algorithms, which often rely on empirical rules and trial-and-error strategies to find a network architecture that balances complexity and flexibility. Furthermore, our comparative analysis highlights the superior performance of SVR over established models such as WS* and HBF25 [9], particularly in extrapolating charge radii towards the driplines. The notable agreements between SVR predictions and experimental data underscore the model's robustness and accuracy across diverse mass regions. These results reaffirm the utility of SVR in advancing our understanding of nuclear charge radius properties and its potential applications in nuclear physics research.

Data availability statement

All data that support the findings of this study are included within the article (and any supplementary files).

Acknowledgments

This work is supported by the National Natural Science Foundation of China (Grant No. 12250410254), the ZSTU intramural grant (Grant No. 23062211-Y) and Natural Science Foundation of Tianjin (20JCYBJC01510).

ORCID iDs

Amir Jalili https://orcid.org/0000-0002-0280-3427
Ai-Xi Chen https://orcid.org/0000-0002-7953-3752

References

[1] Weizsäcker C V 1935 *Z. Phys.* **96** 431
[2] Duflo J 1994 *Nucl. Phys.* A **576** 29
[3] Piekarewicz J, Centelles M, Roca-Maza X and Vinas X 2010 *Eur. Phys. J.* A **46** 379
[4] Wang N and Li T 2013 *Phys. Rev.* C **88** 011301
[5] Sheng Z, Fan G, Qian J and Hu J 2015 *Eur. Phys. J.* A **51** 40
[6] Bao M, Zong Y, Zhao Y and Arima A 2020 *Phys. Rev.* C **102** 014306
[7] Li T, Luo Y and Wang N 2021 *At. Data Nucl. Data Tables* **140** 101440
[8] An R, Jiang X, Cao L-G and Zhang F-S 2022 *Phys. Rev.* C **105** 014325
[9] Goriely S, Chamel N and Pearson J 2013 *Phys. Rev.* C **88** 024308
[10] Stoitsov M V, Dobaczewski J, Nazarewicz W, Pittel S and Dean D J 2003 *Phys. Rev.* C **68** 054312
[11] Ma C, Zong Y Y, Zhao Y M and Arima A 2021 *Phys. Rev.* C **104** 014303
[12] Sun B-H, Liu C-Y and Wang H-X 2017 *Phys. Rev.* C **95** 014307
[13] Zheng R-Y, Sun X-X, Shen G-f and Geng L-S 2024 *Chin. Phys.* C **48** 014107
[14] Zhang X, Niu Z, Sun W and Xia X 2023 *Phys. Rev.* C **108** 024310
[15] Zhang K *et al* 2022 *At. Data Nucl. Data Tables* **144** 101488
[16] Goriely S, Chamel N and Pearson J M 2016 *Phys. Rev.* C **93** 034337
[17] Choudhary P, Srivastava P C and Navrátil P 2020 *Phys. Rev.* C **102** 044309
[18] Forssén C, Caurier E and Navrátil P 2009 *Phys. Rev.* C **79** 021303
[19] Angeli I and Marinova K P 2013 *At. Data Nucl. Data Tables* **99** 69
[20] Engfer R, Schneuwly H, Vuilleumier J, Walter H and Zehnder A 1974 *At. Data Nucl. Data Tables* **14** 509
[21] Fricke G, Bernhardt C, Heilig K, Schaller L, Schellenberg L, Shera E and Dejager C 1995 *At. Data Nucl. Data Tables* **60** 177
[22] Garcia Ruiz R F *et al* 2016 *Nat. Phys.* **12** 594
[23] Rosenbusch M *et al* 2015 *Phys. Rev. Lett.* **114** 202501
[24] Marsh B A *et al* 2018 *Nat. Phys.* **14** 1163
[25] Miller A J *et al* 2019 *Nat. Phys.* **15** 432
[26] Tang L and Zhang Z-H 2024 *Nucl. Sci. Tech.* **35** 19
[27] Dong X-X, An R, Lu J-X and Geng L-S 2023 *Phys. Lett.* B **838** 137726
[28] Cao Y-Y, Guo J-Y and Zhou B 2023 *Nucl. Sci. Tech.* **34** 152
[29] Dong X-X, An R, Lu J-X and Geng L-S 2022 *Phys. Rev.* C **105** 014308
[30] Wu D, Bai C, Sagawa H and Zhang H 2020 *Phys. Rev.* C **102** 054323
[31] Zeng L-X, Yin Y-Y, Dong X-X and Geng L-S 2024 *Phys. Rev.* C **109** 034318
[32] Yang Z-X, Fan X-H, Naito T, Niu Z-M, Li Z-P and Liang H 2023 *Phys. Rev.* C **108** 034315
[33] Munoz J M, Akkoyun S, Reyes Z P and Pachon L A 2023 *Phys. Rev.* C **107** 034308
[34] Li W, Zhang X, Niu Y and Niu Z 2023 *J. Phys. G: Nucl. Part. Phys.*
[35] Molchanov O M, Launey K D, Mercenne A, Sargsyan G H, Dytrych T and Draayer J P 2022 *Phys. Rev.* C **105** 034306
[36] Wang Y, Zhang X, Niu Z and Li Z 2022 *Phys. Lett.* B **830** 137154
[37] Saxena G, Sharma P and Saxena P 2021 *J. Phys. G: Nucl. Part. Phys.* **48** 055103
[38] Niu Z, Liang H, Sun B, Long W and Niu Y 2019 *Phys. Rev.* C **99** 064307
[39] Niu Z and Liang H 2018 *Phys. Lett.* B **778** 48
[40] Utama R, Piekarewicz J and Prosper H 2016 *Phys. Rev.* C **93** 014311
[41] Utama R, Chen W-C and Piekarewicz J 2016 *J. Phys. G: Nucl. Part. Phys.* **43** 114002
[42] Wu X, Lu Y and Zhao P 2022 *Phys. Lett.* B **834** 137394
[43] Wang N and Liu M 2011 *Phys. Rev.* C **84** 051303
[44] Niu Z, Zhu Z, Niu Y, Sun B, Heng T and Guo J 2013 *Phys. Rev.* C **88** 024325
[45] Vapnik V 1999 *The Nature of Statistical Learning Theory (Springer Science and Business Media)*
[46] Cortes C and Vapnik V 1995 *Mach. Learn.* **20** 273
[47] Haykin S 1999 *Neural Networks: A Comprehensive Foundation* 2nd edn (McMillan)
[48] Angeli I 2004 *At. Data Nucl. Data Tables* **87** 185
[49] Geng L, Toki H and Meng J 2005 *Prog. Theor. Phys.* **113** 785
[50] Nerlo-Pomorska B and Pomorski K 1994 *Z. Phys.* A **348** 169
[51] Bayram T, Akkoyun S, Kara S and Sinan A 2013 *Acta Phys. Pol.* B **44** 1791
[52] Schölkopf B and Smola A J 2002 *Learning With Kernels: Support Vector Machines, Regularization, Optimization and Beyond* (MIT Press)
[53] Evaluated Nuclear Structure Data File (available at: www.nndc.bnl.gov/nds/)
[54] Ma J-Q and Zhang Z-H 2022 *Chin. Phys.* C **46** 074105
[55] Geldhof S *et al* 2022 *Phys. Rev. Lett.* **128** 152501
[56] Satula W, Bentley M, Jalili A and Uthayakumaar S 2023 *Phys. Rev.* C **108** 044315
[57] Erler J, Birge N, Kortelainen M, Nazarewicz W, Olsen E, Perhac A M and Stoitsov M 2012 *Nature* **486** 509–12
[58] Afanasjev A, Agbemava S, Ray D and Ring P 2013 *Phys. Lett.* B **726** 680–4
[59] Agbemava S E, Afanasjev A V, Ray D and Ring P 2014 *Phys. Rev.* C **89** 054320–37
[60] See Supplemental Material for charge radii prediction based on SVR (extrapolation performance towards driplines)